Perturbative calculation of two-photon double electron ionization of helium.

I. A. Ivanov† and A. S. Kheifets

Research School of Physical Sciences and Engineering, The Australian National University, Canberra ACT 0200, Australia

Abstract. We report the total integrated cross-section (TICS) of two-photon double ionization of helium in the photon energy range from 40 to 54 eV. We compute TICS in the lowest order perturbation theory (LOPT) using the length and Kramers-Henneberger gauges of the electromagnetic interaction. Our findings indicate that the LOPT gives results for TICS in agreement with our earlier non-perturbative calculations.

PACS numbers: 32.80.Rm 32.80.Fb 42.50.Hz

† Corresponding author: Igor.Ivanov@.anu.edu.au

1. Introduction

In recent years, two-photon double-electron ionization (TPDI) of helium has been a subject of considerable interest. A large number of theoretical methods have been developed and applied to this problem. Among them are the lowest order perturbation theory (LOPT) with correlated multichannel states (Nikolopoulos and Lambropoulos 2001), the many-electron many-photon theory (Mercouris *et al* 2001), the R-matrix Floquet approach (Feng and van der Hart 2003), the exterior complex scaling (ECS) method (Horner *et al* 2007), flux formulation (Shakeshaft 2007) and various time-dependent methods (Kamta and Starace 2002, Piraux *et al* 2003, Lambropoulos *et al* 1999, Scrinzi and Piraux 1998, Caillat *et al* 2005, Pindzola and Robicheaux 1998, Colgan and Pindzola 2002, Hu *et al* 2005, Foumouo *et al* 2006, Nikolopoulos and Lambropoulos 2007, Ivanov and Kheifets 2007). The picture which emerged as a result of these studies is somewhat puzzling. Almost all the available theoretical results for the total integrated cross-section (TICS) of TDPI can be categorized into one of two broad groups. One of the groups (below we shall call it group A for brevity) is represented by several methods such as time-dependent close-coupling (TDCC) (Hu *et al* 2005, Colgan and Pindzola 2002), time-dependent basis (Piraux *et al* 2003, Ivanov and Kheifets 2007), R-matrix Floquet (Feng and van der Hart 2003) and ECS (Horner *et al* 2007). These results agree with each other with a typical accuracy of 40% in the interval of photon energies of 40–47 eV where the TICS is a monotonously growing function of the photon energy.

The second group, to which we shall refer as group B, is represented by the LOPT calculation (Nikolopoulos and Lambropoulos 2001) and two time-dependent calculations (Foumouo *et al* 2006, Nikolopoulos and Lambropoulos 2007). These works produced TICS which were several times larger than results of the group A for photon energies near 45 eV. In addition, TICS as calculated by Nikolopoulos and Lambropoulos (2001) was slowly decreasing with the photon energy in the interval of 43–47 eV.

The reason for this discrepancy is unclear. Probably the most difficult part of theoretical description of TPDI is an accurate representation of the final doubly ionized atomic state. It might be tempting therefore to attribute the discrepancy between

the results of groups A and B to different representations of the final states. This simple logic, however, does not work. It was shown, e.g. by Foumouo *et al* (2006) and Nikolopoulos and Lambropoulos (2007), that a complete neglect of correlations in the final state does produce a considerable difference but still not enough to account for the observable difference in TICS values.

It was suggested by Colgan and Pindzola (2002) that two-photon ionization of helium in the vicinity of the photon energy of 45 eV is a process in which the core excitation mechanism plays a very important role. As was observed by Colgan and Pindzola (2002), it was this effect that could be responsible for a considerable difference (reaching a factor of 3) between results obtained by different workers for the cross-section of two-photon single electron ionization in the vicinity of the photon energy of 45 eV. The same remark almost certainly applies to TPDI. The resonant core excitation may be responsible for the observed difference of the TICS values if we suppose that various calculations take this effect into account differently.

This remark can be formulated in the language of the perturbation theory by attributing the difference between the two groups of results to different treatment of the intermediate, but not the final, states. Therefore, a comparison of two calculations using the same set of final states but treating the intermediate states differently would be useful. With this goal in mind, we perform a LOPT calculation of TPDI of He whose results are presented below. We demonstrate in the following that the use of LOPT (at least the version of LOPT which we develop) gives numerical values which are close to our previous non-perturbative results obtained by a numerical solution of the time dependent Schrödinger equation (Ivanov and Kheifets 2007).

The paper is organized as follows. In the next section we give an outline of the theoretical procedure. Then we discuss the numerical results for the TICS of TPDI.

2. Formalism

2.1. Atom-field interaction.

The Hamiltonian of the helium atom placed in the external monochromatic electromagnetic (EM) field is

$$\hat{H} = \hat{H}_{\rm atom} + \hat{H}_{\rm int} \ . \tag{1}$$

Here $\hat{H}_{\rm atom}$ is the Hamiltonian of the field-free helium atom which reads, in atomic units

$$\hat{H}_{\rm atom} = \sum_{i=1}^{2} \frac{\boldsymbol{p}_i^2}{2} - \sum_{i=1}^{2} \frac{2}{r_i} + \frac{1}{r_{12}}. \tag{2}$$

The interaction part $\hat{H}_{\rm int}$ depends on the gauge of the electromagnetic interaction. In the following, we employ the length gauge and the so-called Kramers-Henneberger gauge. The latter gauge is less commonly used in LOPT calculations and we shall therefore give a brief summary of this approach. We follow our earlier works (Ivanov and Kheifets 2005*a*, Ivanov and Kheifets 2005*b*) where we applied this technique to two-photon one electron ionization of hydrogen and helium.

The Kramers-Henneberger (KH) picture of the helium atom interaction with the EM field can be derived from the ordinary minimal coupling Hamiltonian

$$\hat{H}_{\rm int} = -\frac{1}{c} \sum_{i=1}^{2} \left(\hat{\boldsymbol{A}} \cdot \hat{\boldsymbol{p}}_i - \frac{\hat{\boldsymbol{A}}^2}{2c} \right) \tag{3}$$

by means of a canonical transformation (Kramers 1956, Henneberger 1968, Pauli and Fierz 1938) generated by the operator:

$$\hat{T} = -\frac{1}{c} \int_0^t \sum_{i=1}^{2} \hat{\boldsymbol{A}}(\tau) \hat{\boldsymbol{p}}_i \ d\tau + \frac{1}{2c^2} \int_0^t \hat{\boldsymbol{A}}^2(\tau) \ d\tau \ , \tag{4}$$

Here $\hat{\boldsymbol{p}}$ is the momentum operator, $\hat{\boldsymbol{A}}$ is the vector potential operator. We shall assume below that the dipole approximation is valid, so the operator $\hat{\boldsymbol{A}}$ does not depend upon the atomic coordinates.

The atom-EM field interaction Hamiltonian $\hat{H}_{\rm KH} = e^{i\hat{T}} \hat{H}_{\rm min} e^{-i\hat{T}} - \dfrac{\partial \hat{T}}{\partial t}$ in this gauge becomes

$$\hat{H}_{\rm KH} = \hat{H}_{\rm atom} + \hat{H}_{\rm int}^{\rm KH} \ , \tag{5}$$

where $\hat{H}_{\rm atom}$ has the same form as the Hamiltonian (2) while the interaction Hamiltonian becomes:

$$\hat{H}_{\rm int}^{\rm KH} = \sum_{i=1}^{2} \left(\frac{2}{r_i} - \frac{2}{|\boldsymbol{r}_i + \hat{\boldsymbol{\alpha}}|} \right), \tag{6}$$

where $\hat{\boldsymbol{\alpha}} = -\int_0^t \hat{\boldsymbol{A}}(\tau)\, d\tau$, $\hat{\boldsymbol{A}}$ is the quantized vector potential operator.

The matrix elements of operator (6) taken between the states describing the noninteracting atom and the EM field can be obtained either from the known matrix elements of the quantized vector potential operator (Ivanov and Kheifets 2005*b*), or from the known correspondence between the quantum and classical description of the EM field (Ivanov and Kheifets 2005*a*). We introduce a state vector $|a, m\rangle$ where a stands for a set of quantum numbers describing the helium atom and m denotes a number of the field photons. With this notation, in the case of a linearly polarized monochromatic EM field, the formula for the matrix elements reads

$$\left\langle a, n+p \left| \hat{H}_{\rm int}^{\rm KH} \right| b, n \right\rangle = \frac{1}{\pi} \sum_{i=1}^{2} \int_0^{\pi} \cos p\theta \left\langle a \left| \frac{2}{r_i} - \frac{2}{|\boldsymbol{r}_i + \boldsymbol{F}\cos\theta/\omega^2|} \right| b \right\rangle d\theta, \tag{7}$$

where $\boldsymbol{F}$ is a vector directed along the polarization axis z and having the magnitude $F^2/8\pi = n\omega$. The well-known expansion:

$$\frac{1}{\left|\boldsymbol{r} + \boldsymbol{F}\cos\theta/\omega^2\right|} = \sum_{k=0} \sqrt{\frac{4\pi}{2k+1}} \frac{r_<^k}{r_>^{k+1}} [-\mathrm{sign}(\cos\theta)]^k \; Y_{k0}(\boldsymbol{r}), \tag{8}$$

where $r_<$ ($r_>$) is the smaller (greater) of r and $F\cos\theta/\omega^2$ allows for separation of the radial and angular variables in Equation (7).

In the case of TPDI, there are two photons less in the final state of the system than in the initial one. Using operator (6) as a perturbation, we obtain two lowest order amplitudes connecting the initial and final states:

$$M_1 = \left\langle a, n+2 \left| \hat{H}_{\rm int}^{\rm KH} \right| b, n \right\rangle, \tag{9}$$

and

$$M_2 = \sum\!\!\!\!\!\!\int_c \frac{\left\langle a, n+2 \left| \hat{H}_{\rm int}^{\rm KH} \right| c, n+1 \right\rangle \left\langle c, n+1 \left| \hat{H}_{\rm int}^{\rm KH} \right| b, n \right\rangle}{E_a + \omega - E_c + i\epsilon}, \tag{10}$$

In these expressions, a is the initial (ground) state of the helium atom, b is the final doubly ionized atomic state and c is the set of intermediate states for which the

corresponding matrix elements have nonzero values. One should note that, in contrast to the length or velocity gauges, the TPDI process in the KH gauge has a nonzero first order amplitude M_1.

To make a connection with PT expansion in the length or velocity form (which are effectively the expansions in powers of F, the external field strength), we should note the following. It is easy to see from Equation (7) that expansions of both M_1 and M_2 in powers of F contain various powers of F. If we are interested in low fields limit, we can retain only the leading order contributions. This can be easily done using Equation (8) with the following result. The leading order contribution to the amplitude M_2 is obtained if we simply replace in Equation (10) the operator $\hat{H}_{\rm int}^{\rm KH}$ with the operator $\hat{H}_{\rm eff}^{\rm KH} = \dfrac{\boldsymbol{F}}{2\omega^2}\left(\dfrac{\boldsymbol{r}_1}{r_1^3} + \dfrac{\boldsymbol{r}_2}{r_2^3}\right)$, i.e. use the acceleration gauge for EM-atom interaction. The set of intermediate states c in Equation (10) is then the set of all atomic states of P symmetry as in the case of the length or velocity forms. The final state can have either S or D symmetry. Similar conclusions follow from the inspection of Equation (7) for the amplitude M_1. The leading contribution to this amplitude is of the order of F^2 and the final state should be of either S or D symmetry. There is no expression for this amplitude in a simple operator form and we should use Equation (8) to compute it. In practical calculations it is convenient to compute the amplitude M_1 using Equation (8) for sufficiently low values of EM field strength. For $F = 0.03$ a.u. the contribution of the next to the leading order corrections in powers of F to this amplitude is negligible.

For the calculation using the length gauge, the first order amplitude (9) is, of course absent. To compute the second order amplitude we use Equation (10) with the dipole interaction operator $\hat{H}^{\rm L} = \boldsymbol{F}(\boldsymbol{r}_1 + \boldsymbol{r}_2)/2$ instead of $\hat{H}_{\rm eff}^{\rm KH}$.

2.2. Atomic states.

2.2.1. Initial and intermediate states. To carry over summation over all intermediate states in Equation (10) we use the discretization method developed by Cormier and Lambropoulos (1995) and applied to the problem of TPDI of helium by Nikolopoulos and Lambropoulos (2001). Within this procedure, the set of intermediate states in the PT expressions is replaced by the set obtained by diagonalization of the atomic

Hamiltonian in a suitably chosen basis. Below, we use the variant of the discretization procedure described by Cormier and Lambropoulos (1995). The infinite sum in the exression for the second order amplitude (10) is computed as

$$M_2 = \lim_{\epsilon \to 0} \sum_i \frac{\left\langle a \left| \hat{H}_{\rm eff}^{\rm KH} \right| c_i \right\rangle \left\langle c_i \left| \hat{H}_{\rm eff}^{\rm KH} \right| b \right\rangle}{E_a + \omega - E_{c_i} + i\epsilon} \tag{11}$$

where c_i is the discrete set of states resulting from the diagonalization of the atomic Hamiltonian. We dropped the photon numbers in Equation (11) as redundant here and considered only the KH gauge. The calculation in the length gauge employs a similar procedure.

The limit of $\epsilon \to 0$ cannot be taken directly in Equation (11) as for too small values of this parameter the amplitude M_2 may exhibit a divergent behavior. There is, however, an interval of ϵ for which this amplitude is a slowly varying function of this parameter which can be reliably extrapolated to the limit $\epsilon = 0$ (Cormier and Lambropoulos 1995). More details about implementation of this procedure in the present work will be given shortly.

To achieve accurate numerical results, it is necessary to ensure that the density of discrete states c_i is sufficiently large near the position of the pole of the PT expansion. In the present case of TPDI from the ground state of helium for the photon energies in the vicinity of 45 eV, this pole is located at approximately -1 a.u. In this case a sufficiently large density of the states c_i can be achieved if we employ a basis composed of B-spline box states. Such a basis was prepared as follows. We used a set of B-splines of the order $k = 7$ with the knots located at the sequence of points lying in $[0, R_{\rm max}]$ where the size of the box $R_{\rm max}$ was varying between 60 a.u. and 100 a.u. A typical number of knot points was 40-45. All the knots t_i were simple ones except for the knots located at the origin and the outer boundary $R = R_{\rm max}$ of the box. These knots had multiplicity $k = 7$. The simple knots were distributed in $(0, R_{\rm max})$ according to the rule $t_{i+1} = t_i + \beta$. The parameter β was close to 2.

For each value of the angular momentum l the first $l + 1$ B-splines and the last B-spline resulting from this sequence of knots were discarded. The omission of the first $l + 1$ B-splines ensured that any B-spline in the set decreased as r^{l+1} (or faster) at the

origin. The omission of the last B-spline ensured that all B-splines of a set assumed the zero value at the outer boundary. The set of B-splines constructed for each l served as a set of one-electron radial functions $R_l(r)$. The two-electron basis functions with a given value of the total angular momentum were built from the one-electron orbitals with angular momenta $l \leq l_{\max}$ in a usual way. The size of the basis employed in the calculation depends thus upon the box size used and the value of the parameter $l_{\max}$. The two-electron basis functions thus obtained were used both to represent the initial ground S-state of the atom and the set of intermediate P-states in Equation (11). To ensure that our results are stable with respect to the choice of the basis, we shall present below results of calculations which use different values for both these parameters.

2.2.2. Final states. The final states we need for TPDI calculations are the states of the S- and D- symmetry with ingoing boundary conditions describing two electrons in continuum. These states are provided by the convergent close-coupling (CCC) method (Bray 1994). In this method, the two-electron scattering state is represented by a close-coupling expansion over the channel states, each of which is composed of a target pseudostate f and a Coulomb wave $\boldsymbol{k}$:

$$\Psi_f(\boldsymbol{k}) = |\boldsymbol{k}f\rangle + \sum_{\boldsymbol{k}'j} \frac{\langle \boldsymbol{k}f|T|\boldsymbol{k}'j\rangle}{E - k'^2/2 - \varepsilon_j - i0} |\boldsymbol{k}'j\rangle \tag{12}$$

Here $\langle \boldsymbol{k}f|T|\boldsymbol{k}'j\rangle$ is half-on-shell T-matrix which is found by solving a set of coupled Lippmann-Schwinger equations (Bray and Stelbovics 1995). Implicit in Equation (12) is the energy conservation $E_0 + 2\omega = \varepsilon_f + k^2/2$.

The wave functions (12) with positive energy pseudostates $\varepsilon_f > 0$ can be used for description of the two-electron continuum (Bray 1994, Bray and Stelbovics 1995). The radial and angular parts are separated in Equation (12) by the partial wave expansion of the wavefunction

$$\Psi_f(\boldsymbol{k}) = \sum_{\substack{lm \\ JM}} \Psi_{lf(J)}(k) \langle lml_f m_f | JM\rangle Y_{lm}(\hat{\boldsymbol{k}}) \ . \tag{13}$$

Here the angular momenta of the photoelectron l and the pseudostate l_f are coupled to the total angular momentum J. For the present TPDI problem, only the terms in the partial wave expansion with $J = 0, 2$ are needed. For consistency, the largest value

which l_f could assume was chosen to be equal to the parameter $l_{\max}$ introduced above. The results of the calculation presented below were obtained for $l_{\max} = 3$. To make sure that this value is large enough to achieve the convergence of the results, we also report some results obtained for $l_{\max} = 2$.

2.3. Calculation of TICS

In the previous section, we described all the ingredients needed for computing the TPDI amplitudes (9-10). Substituting the final CCC state (12) into these expressions allows to compute the cross section of a process in which absorption of two photons leaves the helium atom in a state with one continuum electron with the momentum k and the target electron described by a pseudostate f. This cross section, in units of cm^{4}s, reads

$$\sigma_f = 2^7\pi^3\alpha^2 a_0^4 \tau\omega^2 \frac{\left|M_1^f + M_2^f\right|^2}{F^4}, \tag{14}$$

where α is the fine structure constant, the Bohr radius $a_0 = 0.529 \times 10^{-8}$ cm and the atomic unit of time $\tau = 2.418 \times 10^{-17}$ s. The CCC wavefunctions representing the final states are normalized to the delta-function of energy. The sum of σ_f over all positive energy pseudostates $\varepsilon_f > 0$ gives us the TICS of TPDI.

3. Results

First, we shall address the issue of stability of the TICS calculation with respect to the choice of the basis set. To illustrate this point, we present in Figures 1 and 2 the TICS values obtained in the KH and length gauges for various values of the ϵ parameter in Equation (11). Results of several calculations using different box sizes and basis compositions are presented. These calculations are labelled as follows. In the calculation a) we used the box size $R_{\max} = 60$ a.u. and $l_{\max} = 3$. This choice gave us 2180 basis states of S-symmetry and 3170 states of P-symmetry. Diagonalization of the field-free helium Hamiltonian using the set of basis states of S-symmetry gave us the ground state with the energy of -2.8872 a.u. which we used as the initial state. The set of the states of the P-symmetry was used as a set of the intermediate states in Equation (11). The calculation b) used $R_{\max} = 80$ a.u. and $l_{\max} = 3$ which gave 3700

basis S-states and 5420 basis P-states. Calculations c), d), and e) all used $l_{\max} = 2$ and the values of $R_{\max} = 60$ a.u., 80 a.u., and 100 a.u. respectively. The basis sizes of these calculations were composed of 1684 S- and 2178 P-states, 2839 S- and 3698 P-states and 4135 S- and 5408 P-states, correspondingly. As we mentioned above, for too small values of ϵ, the discretization rule prescribed by Equation (11) fails and the amplitude may exhibit a divergent behavior. For reliable application of this formula, the parameter ϵ should be several times (two or three) larger than the energy spacing of the dicrete eigenvalues near the pole (Cormier and Lambropoulos 1995). For the calculations described above, this spacing was typically of the order of 0.05 a.u. near the pole. We should, therefore, expect divergent behavior to appear for values of ϵ of the order of 0.1. To see clearly when the regime of the divergent small-ϵ behavior takes place, we adjust the photon frequency in Equation (11) so that $E_a + \omega - E_{c_i} = 0$ for some c_i. Ortherwise, the amplitude given by Equation (11) would remain finite for $\epsilon = 0$, which may mask the inevitable breakdown of the discretization rule for very small values of ϵ. Results reported below were obtained for the photon frequencies thus chosen. For the calculations a)–e) this choice of the photon frequency gives a value near 44.3 eV. The corresponding TICS are shown in Figures 1 and 2.

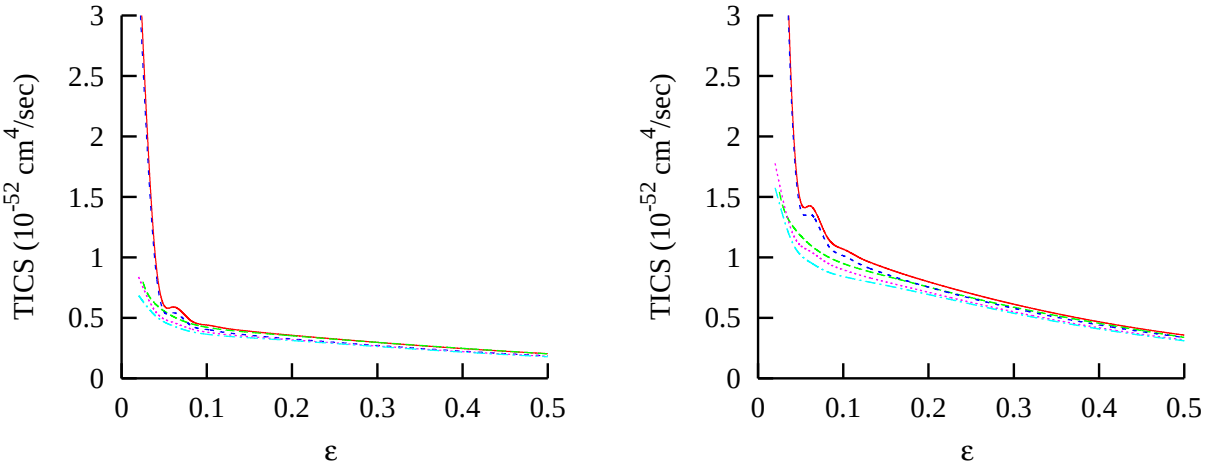

Figure 1. (Color online) Partial S-wave (left panel) and D-wave (right panel) contributions to TICS, in units of 10^{-52} cm^{4}s, as functions of the ϵ parameter for the photon energy ω=44.3 eV. Calculation a) (red) solid; b) (green) dashed; c) (blue) short dashed; d) (magenta) dotted; e) (light blue) dot dashed. All calculations are in the KH gauge.

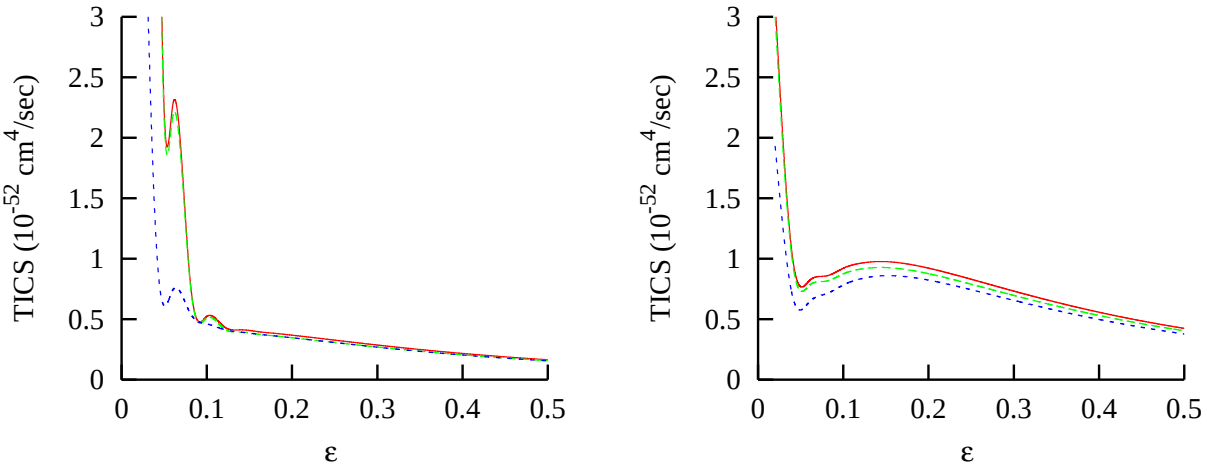

Figure 2. (Color online) Partial S-wave (left panel) and D-wave (right panel) contributions to TICS, in units of 10^{-52} cm^{4}s, as functions of the parameter ϵ for photon energy ω=44.3 eV. Calculation a) (red) solid; b) (green) dashed; c) (blue) short dashed. All calculations are in the length gauge.

As one can see from Figures 1 and 2, the TICS is a monotonous slowly varying function of the ϵ parameter in both gauges for $\epsilon > 0.15$. This means that we can use these data for extrapolation to the limit $\epsilon = 0$. One can also observe that results of all the calculations presented in Figures 1 and 2 are close to each other which means that for $l_{\max} = 2$ we have already achieved a reasonably good convergence with respect to the total number of one-electron angular momentum states included in the calculation. Also, these calculations are well converged with respect to the the size of the box $R_{\max}$. These latter features show that we can expect to achieve good accuracy for TICS calculations. It is these two features that also make the calculation possible at all since the basis size grows very rapidly with $R_{\max}$ and $l_{\max}$. Having in mind these observations concerning the convergence of the calculation, we shall consider the results of the calculation a) ($R_{\max} = 60$ a.u.; $l_{\max} = 3$) as our final results. Another indicator of the accuracy of the calculation is agreement of the results obtained in different gauges. This point is illustrated in Figure 3 the where KH and length gauge results are shown for the photon energy of 48.33 eV.

One can see from Figure 3 that, just as for the photon energy of 44.3 eV, the KH and length gauge results for 48.33 eV are sufficiently close to each other and for $\epsilon > 0.15$

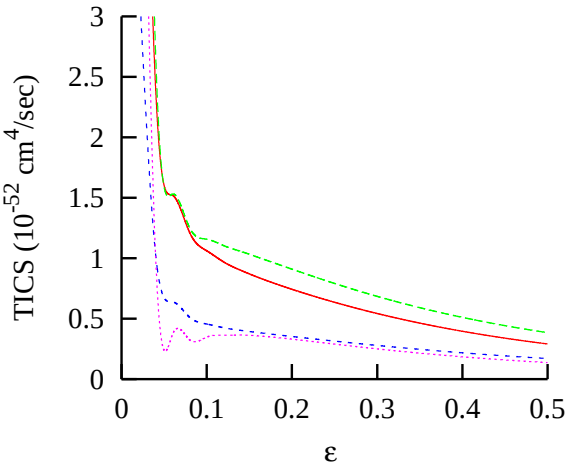

Figure 3. (Color online) Partial S-wave and D-wave contributions to TICS, in units of 10^{-52} cm^{4}s, as functions of the ϵ parameter for photon energy ω=48.33 eV. Calculation a); D-wave, the KH gauge (red) solid; D-wave, the length gauge (green) dashed; S-wave, the KH gauge (blue) short dashed; S-wave length gauge (magenta) dotted.

the TICS is a slowly varying monotonous functions of ϵ enabling reliable extrapolation to the $\epsilon \to 0$ limit. This feature was also confirmed for all other photon energies reported below. The summary of the extrapolated results (in both gauges) is given in the Table 1 below. To be able to attest the accuracy of extrapolalation to $\epsilon \to 0$ we present results of two extrapolation procedures: quadratic and cubic (extrapolating to $\epsilon = 0$ from the region $\epsilon > 0.2$ by the 2-nd and 3-rd order polinomial fitin ϵ, respectively).

Table 1. Quadratic and cubic (in parentheses) extrapolation of the partial D- and S-wave contributions to TICS, in units of 10^{-52} cm^{4}s, in the length and KH gauges for various photon energies.

ω (a.u.)	D-wave	S-wave	D-wave	S-wave
	Length gauge		KH gauge	
40.85	0.638 (0.700)	0.404 (0.376)	0.640 (0.631)	0.234 (0.231)
42.5	1.051 (1.148)	0.679 (0.601)	0.948 (0.986)	0.363 (0.387)
44.3	1.001 (1.312)	0.472 (0.563)	1.282 (1.305)	0.482 (0.489)
48.33	1.470 (1.549)	0.461 (0.543)	1.337 (1.348)	0.510 (0.539)
50.6	2.959 (2.912)	1.128 (1.088)	2.314 (2.237)	0.970 (0.967)
53	7.482 (5.763)	3.550 (2.669)	5.579 (4.220)	2.518 (1.933)

Each entry of the table represents the results of extrapolation of the calculation a) to the $\epsilon = 0$ limit for various photon energies in the interval of 40-53 eV. For each entry we present results of the quadratic and cubic (in parenthesis) extrapolation. As one can

see, except for the entries for 53 eV, the different extrapolation procedures give variation of the results of the order of a few percent for the KH gauge, and of the order of 25% for the length gauge. The difference between the KH and length gauges results (again, except for the values for 53 eV) is also of the order of 25%. We can adopt this figure as a conservative estimate of the uncertainty of our calculation. Our feeling is that the KH results are probably considerably more accurate than the length ones. This feeling is based on the observation that in the KH gauge the field-atom interaction goes to zero at large distances which makes it, perhaps, a better tool for the problem at hand. In particular, we can expect a better convergence of the KH gauge calculation with the box size. Also, as Table 1 shows, the KH gauge results are much less sensitive to the extrapolation procedure we choose. We would be inclined to believe, therefore, that the accuracy of the KH gauge results might be higher than the above estimate of 25%.

The KH results with the quadratic extrapolation are plotted in Figure 4 together with our previous non-perturbative time-dependent calculation and other group A and B results. As is seen from Figure 4, the present calculation is in much better agreement with the group A results than the group B. Together with the flux formula calculation of Shakeshaft (2007), it can be seen as an "upper boundary" of the group A. The TDCC (Hu *et al* 2005) and ECS (Horner *et al* 2007) results form the "lower boundary" of this group.

4. Conclusion.

In the present work, we studied two-photon double electron ionization of helium in the photon energy range from 40 eV to the energies close to the threshold of the sequential ionization at 54.4 eV. Our calculation had two purposes. More utilitarian one was to confirm (or otherwise) our previous non-perturbative result (Ivanov and Kheifets 2007) and, more broadly, to test the consensus built around the cluster of works which we categorized into the group A. We believe that we achieved this purpose: the LOPT calculation seems to be sufficiently accurate. As we saw, the LOPT calculations, both in the length and Kramers-Henneberger gauges, are quite stable with respect to variation of the parameters ($R_{\max}$, $l_{\max}$) determining the basis size. The results of the calculations

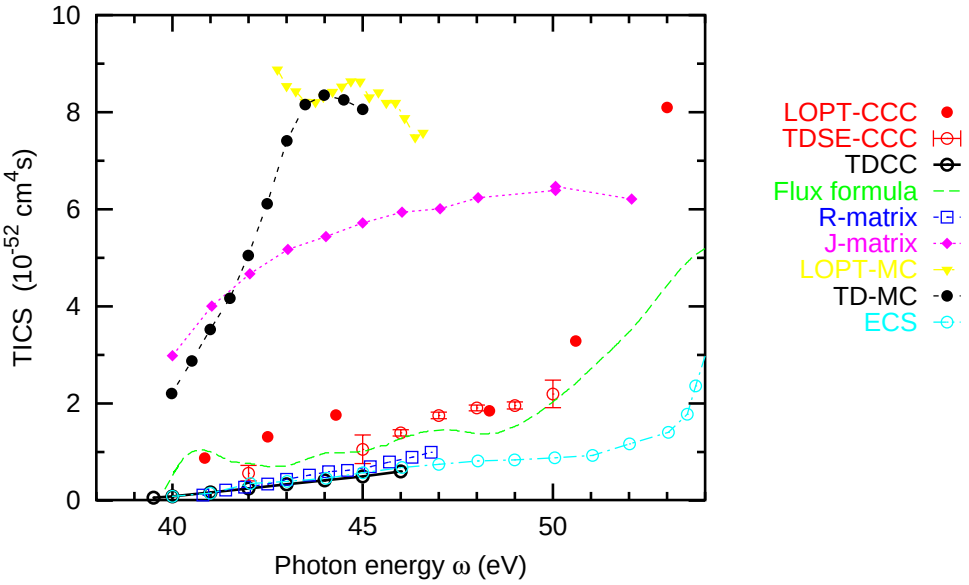

Figure 4. (Color online) Total integrated cross-section of TPDI of He as a function of the photon energy. Present LOPT results with the CCC final state are shown by (red) filled circles. Our earlier results (Ivanov and Kheifets 2007) obtained by solving the time-dependent Schrödinger equation (TDSE) and projecting on the CCC final state are shown by (red) open circles. Other calculations are as follows: time-dependent close-coupling (TDCC) (Hu *et al* 2005) , open (black) circles; flux formula (Shakeshaft 2007), (green) dash; *R*-matrix (Feng and van der Hart 2003), (blue) open squares; *J*-matrix (Foumouo *et al* 2006), (purple) filled diamonds; LOPT with multichannel (MC) states (Nikolopoulos and Lambropoulos 2001), (yellow) filled triangles, TD calculation with multichannel states (Nikolopoulos and Lambropoulos 2007), (black) filled circles; exterior complex scaling (ECS) (Horner *et al* 2007), (light blue) open circles.

using different gauges agree generally within 25% with each other which can be accepted as an accuracy estimate of the present calculation. Our results with this accuracy margin confirm our previous non-perturbative calculation (Ivanov and Kheifets 2007) and lend support to the group A theories.

On a more fundamental level, the fact that LOPT is capable to describe TDPI in helium quite well seems to us rather important. As we mentioned in the Introduction the suggestion, that the difference of the results between groups A and B is due to different treatment of electron correlations in the final state, has been disproved. We might then turn our attention to the intermediate states of the process. Presence of strong resonant effects in the problem might explain the difference of the results if, for some reason, not all theoretical methods were capable to describe these effects equally well. Our results indicate that no such effects are inherent to this problem. As to a

large discrepancy between the group A and B results, the answer to this still intriguing question must be looked elsewhere.

5. Acknowledgements

The authors acknowledge support of the Australian Research Council in the form of the Discovery grant DP0771312. Facilities of the Australian Partnership for Advanced Computing (APAC) were used. The authors are thankful to Fernando Martín for communicating his results prior to publication.

Bray I 1994 *Phys. Rev. A* **49**(2), 1066–1082
Bray I and Stelbovics A T 1995 *Adv. Atom. Mol. Phys.* **35**, 209
Caillat J, Zanghellini J, Kitzler M, Koch O, Kreuzer W and Scrinzi A 2005 *Phys. Rev. A* **71**, 012712
Colgan J and Pindzola M S 2002 *Phys. Rev. Lett.* **88**, 173002
Cormier E and Lambropoulos P 1995 *jpb* **28**, 5043
Feng L and van der Hart H W 2003 *J. Phys. B* **36**(1), L1–L7
Foumouo E, Kamta G L, Edah G and Piraux B 2006 *Phys. Rev. A* **74**, 063409
Henneberger W C 1968 *Phys. Rev. Lett.* **21**, 838
Horner D A, Morales F, Rescigno T N, Martin F and McCurdy C W 2007 *Phys. Rev. A* **76**(3), 030701
Hu S X, Colgan J and Collins L A 2005 *J. Phys. B* **38**, L35
Ivanov I A and Kheifets A S 2005*a* *J. Phys. B* **38**, 2245
Ivanov I A and Kheifets A S 2005*b* *Phys. Rev. A* **71**, 043405
Ivanov I A and Kheifets A S 2007 *Phys. Rev. A* **75**, 033411
Kamta G L and Starace A F 2002 *Phys. Rev. A* **65**, 053418
Kramers H A 1956 *Collected Scientific Papers* North Holland Amsterdam
Lambropoulos P, Maragakis P and Zhang J 1999 *Phys. Rep.* **305**, 203
Mercouris T, Haritos C and Nicolaides C A 2001 *J. Phys. B* **34**, 3789
Nikolopoulos L A A and Lambropoulos P 2001 *J. Phys. B* **34**, 545
Nikolopoulos L A A and Lambropoulos P 2007 *J. Phys. B* **40**(6), 1347
Pauli W and Fierz M 1938 *Nuovo Cimento* **15**, 167
Pindzola M S and Robicheaux F 1998 *J. Phys. B* **31**(19), L823–L831
Piraux B, Bauer J, Laulan S and Bachau H 2003 *Eur. Phys. J. D* **26**, 7
Scrinzi A and Piraux B 1998 *Phys. Rev. A* **58**, 1310
Shakeshaft R 2007 *Phys. Rev. A* **76**(6), 063405